International Journal of Chemical, Materials and Biomolecular Sciences
ISSN: 2415-6620
Vol:10, No:2, 2016

Microstructure and Electrochemical Properties of $LiNi_{1/3}Co_{1/3}Mn_{1/3-x}Al_xO_2$ Cathode Material for Lithium Ion Batteries

Wei-Bo Hua, Zhuo Zheng, Xiao-Dong Guo, Ben-He Zhong

***Abstract*—**The layered structure $LiNi_{1/3}Co_{1/3}Mn_{1/3-x}Al_xO_2$ ($x = 0 \sim 0.04$) series cathode materials were synthesized by a carbonate co-precipitation method, followed by a high temperature calcination process. The influence of Al substitution on the microstructure and electrochemical performances of the prepared materials was investigated by X-Ray diffraction (XRD), scanning electron microscopy (SEM), and galvanostatic charge/discharge test. The results show that the $LiNi_{1/3}Co_{1/3}Mn_{1/3-x}Al_xO_2$ has a well-ordered hexagonal α-$NaFeO_2$ structure. Although the discharge capacity of Al-doped samples decreases as x increases, $LiNi_{1/3}Co_{1/3}Mn_{1/3-0.02}Al_{0.02}O_2$ exhibits superior capacity retention at high voltage (4.6 V). Therefore, $LiNi_{1/3}Co_{1/3}Mn_{1/3-0.02}Al_{0.02}O_2$ is a promising material for "green" vehicles.

***Keywords*—**Lithium ion battery, carbonate co-precipitation, microstructure, electrochemical properties.

I. Introduction

LITHIUM-ION batteries (LIBs) have been considered as the most attractive power source because of their high energy density, high voltage, and long cycle life [1]. $LiCoO_2$ has been the most widely used positive electrode material since it was commercialized by Sony in 1991 [2]. Its further development, however, is seriously restricted by the toxicity, high cost, and instability, etc. [3], [4] So, the $LiNi_{1/3}Co_{1/3}Mn_{1/3}O_2$, which was first reported by Ohzuku's research group in 2001, has attracted enormous attention due to its stable cycleability, safety, and high discharge capacity [5]-[11]. As far as we know, the $LiNi_{1/3}Co_{1/3}Mn_{1/3}O_2$ is one of the most promising candidates to replace $LiCoO_2$ cathode materials for LIBs [12]. In order to meet the requirements of the large-scale high-power system such as the electric vehicles (EVs), nevertheless, it is still a challenge to improve the structural stability and specific energy at high power rate and high voltage as the cycle properties and rate capability of this material become seriously deteriorated when charged to 4.6 V [12], [13]. Therefore, much research has been performed to optimize this series material by novel synthesis routes, using coating and employing metal substituted for Ni, Co and/or Mn [2], [14]-[24].

It is well-acknowledged that Al substitutions have a great impact on the cycle performance of layered lithium transition metal oxides [25], [26]. Dahn, J. R and other groups have confirmed that the thermal stability of Al-substituted layered lithium transition metal oxides, such as $LiNi_{1/3}Mn_{1/3}Co_{(1/3-z)}Al_zO_2$ [27], [28], $LiNi_{1/3}Mn_{1/3}Al_{(1/3-x)}Co_xO_2$ [29], $LiNi_{0.5-z}Mn_{0.5-z}Al_{2z}O_2$ [30], $Li_{1-x}(Ni_{0.40}Mn_{0.40}Co_{0.2-z}Al_z)_{1-x}O_2$ [31], increases with increasing content of Al. Noted that Al in previous researches is usually employed to substitute part of Co. We are especially interested in substitution of Al for Mn, because the valence state of Al is lower than Mn, which may has a positive effect on the Li-ion diffusion. According to our knowledge, Al^{3+} substituted for Mn^{4+} in $LiNi_{1/3}Co_{1/3}Mn_{1/3}O_2$ has been reported [32], however, there has been no report about the advanced electrochemical properties at high voltage, especially high rate capabilities.

Wei-Bo Hua, Zhuo Zheng, Xiao-Dong Guo, Ben-He Zhong are with the College of Chemical Engineering, Sichuan University, Chengdu 610065, China. (phone: +86-28-85406702; fax: +86-28-85406702; e-mail: zhongbenhe@163.com).

II. Experimental

A. Material Preparation

All chemical reagents were of analytical purity and used without further purification. Firstly, a Na_2CO_3 and NH_4HCO_3 aqueous solution (molar ratio = 1:1) and a mixed solution of $Ni(NO_3)_2 \cdot 6H_2O$, $Co(NO_3)_2 \cdot 6H_2O$, $Mn(Ac)_2 \cdot 4H_2O$ and $Al(NO_3)_3 \cdot 9H_2O$ were simultaneously added drop-wisely to a batch reactor using a two-channel peristaltic pump. The molar ratio of Ni: Co: Mn: Al was 1: 1: (1-3x): 3x. The temperature, pH, and stirring speed are respectively controlled in 50-60°C, 8–9 and 800-1000 rpm. The carbonate precursors were filtered and washed thoroughly by centrifuging, and then was dried at 90°C overnight. The obtained powder and an appropriate of lithium carbonate were mixed completely by high energy mechanical milling. Lastly, the mixtures were firstly preheated at 500°C for 6 h to melt the lithium salt, then calcined at 900°C for 10 h in air. The products (x = 0.00, 0.01, 0.02, 0.03, 0.04) were denoted as Al 0, Al 1, Al 2, Al 3, Al 4, respectively.

B. Materials Characterization

The powder X-ray diffraction was made by using a Philip-produced PW 1730 diffractometer. XRD data were collected in the 2θ between 10° and 70° with a scanning speed of 0.06° s^{-1}. Unit cell parameters were refined by the Rietveld method using the Jade 5.0 program. The scanning electron microscopy (SEM) was used to observe the morphology and particle size of the materials (S4800 machine).

C. Electrochemical Measurements

The electrochemical characterizations were tested in CR2032 coin type half-cell, which was comprised of a cathode, a lithium metal anode, a piece of porous polypropylene film and

an electrolyte. The positive electrode materials contained an active material, carbon black, and PVDF binder in the weight ratio 80:13:7. The electrolyte employed to be analyzed was 1 mol L^{-1} $LiPF_6$ solution in an EC-DMC (1:1 by volume) mixture. The fabricated coin cells were cycled at different current density between 3.0 – 4.6 V (vs Li/Li^+) at room temperature. In this study, the capacity of 180 mA g^{-1} was assumed to the 1 C ratio capacity.

III. Results and Discussions

Fig. 1 shows the XRD patterns of the $LiNi_{1/3}Co_{1/3}Mn_{1/3-x}Al_xO_2$ ($x = 0 \sim 0.04$) samples in the scattering angle range from 10 to 70°. All of the peaks can be indexed to the hexagonal α -$NaFeO_2$ structure ($R\bar{3}m$ space group) and no impurity peaks are detected. It demonstrates that the $LiNi_{1/3}Co_{1/3}Mn_{1/3-x}Al_xO_2$ series are phase pure materials in the range of $x = 0.00 \sim 0.04$. In XRD patterns, the (006) / (102) and (108) / (110) doublet peaks are evidently split, which suggest a well-ordered layered structure [8], [19]. It should be noted that the (108) and (110) peaks become less sharp as x increases. The integrated intensity ratio of (003) and (104) peak is regarded as a measurement of the cation mixing in the layered structure. Because the radius of Li^+ ($r_{Li^+} = 0.76$ Å) is approximate to the radius of Ni^{2+} ($r_{Ni^{2+}} = 0.69$ Å), the transition metal ions (Ni^{2+}) at the 3a sites are could easily enter into the lithium metals at 3b sites. Ni^{2+} ions entering octahedral Li^+ sites will produce NiO phase, which could weakens the intensity of the (003) peak but has no influence on (104) peak [33]. Thus, as the cation mixing is increased, the ratio of I_{003}/I_{104} is decreased. In General, undesirable cation mixing happens when I_{003}/I_{104} value is less than 1.2. Table I lists I_{003}/I_{104} value of $LiNi_{1/3}Co_{1/3}Mn_{1/3-x}Al_xO_2$ series, which are much larger than 1.2 for all samples. It can be observed that a small amount of Al substitution for Mn ($x \leq 0.02$) could restrain the cation mixing to some extent, especially when $x = 0.02$. Table I also gives the lattice parameters and structural parameters. The lattice parameters a, c and unit cell volume decreases monotonously with x increases because the radius of Al^{3+} ($r_{Al^{3+}} = 0.50$ Å) is smaller than that of Mn^{4+} ($r_{Mn^{4+}} = 0.53$ Å) [16]. The value of c/a, however, is the highest when $x = 0.02$, which indicates that $LiNi_{1/3}Co_{1/3}Mn_{1/3-0.02}Al_{0.02}O_2$ owns a better ordered hexagonal layered structure than other samples. Above all, we believe that Al has been incorporated successfully into the layered oxides crystal and Al 2 sample may deliver superior electrochemical properties.

TABLE I
Lattice Parameters and Structural Parameters for $LiNi_{1/3}Co_{1/3}Mn_{1/3-x}AL_xO_2$ Samples

Samples	a (Å)	c (Å)	c/a	I_{003}/I_{104}	Unit cell volume (Å^3)
Al 0	2.8566	14.2206	4.9782	1.43	101.19
Al 1	2.8557	14.2178	4.9787	1.48	100.69
Al 2	2.8550	14.2150	4.9789	1.53	100.55
Al 3	2.8534	14.2033	4.9777	1.47	100.10
Al 4	2.8524	14.1955	4.9767	1.44	99.52

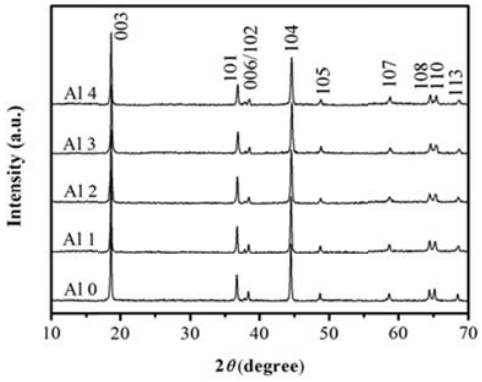

Fig. 1 XRD patterns of $LiNi_{1/3}Co_{1/3}Mn_{1/3-x}Al_xO_2$ samples (10 – 70°)

The surface morphology of the samples were observed using SEM, as shown in Fig. 2. The samples in Fig. 2 display extremely fine crystallites with spherical or polyhedral morphology, an average primary particle sizes are ~ 150 nm, and some of which are agglomerated into a bulk. The primary particle morphologies are similar for all prepared samples, but the particle agglomeration is seemingly aggravated as Al content increases, which are in accordance with the previous report [28], [34]. In general, the regular morphology of prepared particles is beneficial to the electrochemical performances.

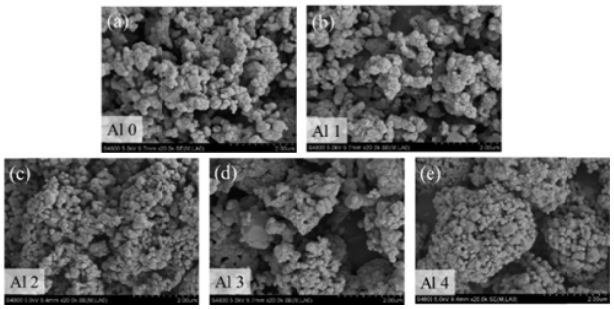

Fig. 2 SEM images of $LiNi_{1/3}Co_{1/3}Mn_{1/3-x}Al_xO_2$ samples

In order to study the impact of Al substitution on the electrochemical properties, the cells were first galvanostatically charged to 4.6 V and subsequently discharged to 3.0 V at a current density of 0.1 C (1 C = 180 mA g^{-1}) under room temperature. Fig. 3 shows the curves of specific discharge capacity vs cycle number for $Li/LiNi_{1/3}Co_{1/3}Mn_{1/3-x}Al_xO_2$ cells. Although Al 0 sample delivers the highest discharge capacity of 139.96 mAh g^{-1} at 1 C, it suffers from a significant capacity drop during cycling and the capacity retention is 87.87% after 50 cycles. The poor cycling performances at high voltage mainly result from the structural instability, oxygen loss from the overlithiated oxide and side reaction caused by HF [2], [8], [25]. On the contrary, the Al doped electrodes exhibit superior cycleability though they own lower initial specific capacity. Among the Al doped samples, Al 2 shows the highest discharge capacity and has few capacity decrease during cycling. The initial discharge capacity is 136.17 mAh g^{-1}, and the capacity retention reaches 99.10% at the 50th cycle. Furthermore, the

specific capacity of Al 2 exceeds that of Al 0 after 15 cycles. In addition, after 50 cycles, the capacity retention of Al 3 and Al 4 are 99.49% and 99.07%, respectively. The results confirm that Al constitution can efficiently enhance the cycling performance of materials.

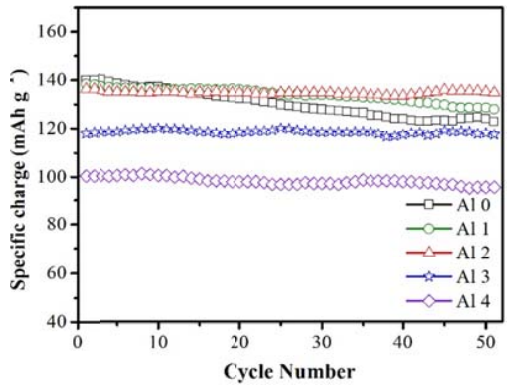

Fig. 3 Specific discharge capacity vs cycle number curves of $Li/LiNi_{1/3}Co_{1/3}Mn_{1/3-x}Al_xO_2$ cells in the potential range of 3.0 – 4.6 V at 1 C

IV. Conclusion

Al substituted layered $LiNi_{1/3}Co_{1/3}Mn_{1/3-x}Al_xO_2$ ($x = 0 \sim 0.04$) materials were successfully synthesized via a co-precipitation and annealing process. All samples have a hexagonal α-$NaFeO_2$ structure and no impurity phases are formed. As the Al content increases, the lattice parameters *a*, *c* and unit cell volume decrease correspondingly. The $LiNi_{1/3}Co_{1/3}Mn_{1/3-x}Al_xO_2$ materials show good cycling performance at high voltage. The Al-free sample has higher initial capacity, but shows inferior cycleability than Al-doped samples. The $LiNi_{1/3}Co_{1/3}Mn_{1/3-0.02}Al_{0.02}O_2$ (Al 2) material delivers an initial discharge capacity of 136.17 mAh g^{-1} between 3.0 and 4.6 V at 1 C rate, and the capacity retention ratio after 50 cycles is 99.10 %. The superior electrochemical performances along with the better thermal stability of Al 2 make it a promising high power positive electrode material for lithium ion batteries.

Acknowledgements

This work was supported by the National Natural Science Foundation of China (Grant No. 21506133), the Science and Technology Pillar Program of Sichuan Province (2014GZ0077).

References

[1] Y.K. Sun, D.H. Kim, C.S. Yoon, S.T. Myung, J. Prakash, K. Amine, A Novel Cathode Material with a Concentration-Gradient for High-Energy and Safe Lithium-Ion Batteries, Adv. Funct. Mater., 20 (2010) 485-491.

[2] W. Luo, X. Li, J.R. Dahn, Synthesis, Characterization, and Thermal Stability of $Li(Ni_{1/3}Mn_{1/3}Co_{1/3-z}(MnMg)_{z/2})O_2$, Chem. Mater., 22 (2010) 5065-5073.

[3] J.N. Reimers, J.R. Dahn, Electrochemical and In Situ X-Ray Diffraction Studies of Lithium Intercalation in Li_xCoO_2, J. Electrochem. Soc., 139 (1992) 2091-2097.

[4] M. Me´ne´trier, I. Saadoune, S.n.p. Levasseur, C. Delmas, The insulator–metal transition upon lithium deintercalation from $LiCoO_2$: electronic properties and Li NMRstudy, J. Mater. Chem., 9 (1999) 1135-1140.

[5] T. Ohzuku, Y. Makimura, Layered Lithium Insertion Material of $LiCo_{1/3}Ni_{1/3}Mn_{1/3}O_2$ for Lithium-Ion Batteries, Chem. Lett., (2001) 642-643.

[6] Y.-S. Hea, Z.-F. Maa, X.-Z. Liaoa, Y. Jiang, Synthesis and characterization of submicron-sized $LiCo_{1/3}Ni_{1/3}Mn_{1/3}O_2$ by a simple self-propagating solid-state metathesis method, Journal of Power Sources 163 (2007) 1053-1058.

[7] T. Mei, Y. Zhu, K. Tang, Y. Qian, Synchronously synthesized core–shell $LiCo_{1/3}Ni_{1/3}Mn_{1/3}O_2$/carbon nanocomposites as cathode materials for high performance lithium ion batteries, RSC Advances, 2 (2012) 12886.

[8] K. Yin, W. Fang, B. Zhong, X. Guo, Y. Tang, X. Nie, The effects of precipitant agent on structure and performance of $LiCo_{1/3}Ni_{1/3}Mn_{1/3}O_2$ cathode material via a carbonate co-precipitation method, Electrochim. Acta, 85 (2012) 99-103.

[9] S.-C. Yin, Y.-H. Rho, I. Swainson, L. F. Nazar*, X-ray/Neutron Diffraction and Electrochemical Studies of Lithium De/Re-Intercalation in $Li_{1-x}Co_{1/3}Ni_{1/3}Mn_{1/3}O_2$ (x= 0 to 1), Chem. Mater., 18 (2006) 1901-1910.

[10] S.H. Ju, Y.C. Kang, The characteristics of Ni–Co–Mn–O precursor and $Li(Ni_{1/3}Co_{1/3}Mn_{1/3})O_2$ cathode powders prepared by spray pyrolysis, Ceramics International, 35 (2009) 1205-1210.

[11] K.M. Shaju, P.G. Bruce, Macroporous $Li(Ni_{1/3}Co_{1/3}Mn_{1/3})O_2$: A High-Power and High-Energy Cathode for Rechargeable Lithium Batteries, Adv. Mater., 18 (2006) 2330-2334.

[12] X. Bie, F. Du, Y. Wang, K. Zhu, H. Ehrenberg, K. Nikolowski, C. Wang, G. Chen, Y. Wei, Relationships between the crystal/interfacial properties and electrochemical performance of $LiNi_{0.33}Co_{0.33}Mn_{0.33}O_2$ in the voltage window of 2.5–4.6V, Electrochim. Acta, 97 (2013) 357-363.

[13] B. Xu, D. Qian, Z. Wang, Y.S. Meng, Recent progress in cathode materials research for advanced lithium ion batteries, Materials Science and Engineering: R: Reports, 73 (2012) 51-65.

[14] S.-T. Myung, S. Komaba, K. Hosoya, N. Hirosaki, Y. Miura, N. Kumagai, Synthesis of LiNi0.5Mn0.5-xTixO2 by an Emulsion Drying Method and Effect of Ti on Structure and Electrochemical Properties, Chem. Mater. , 17 (2005) 2427-2435.

[15] W. Luo, F. Zhou, X. Zhao, Z. Lu, X. Li, J.R. Dahn, Synthesis, Characterization, and Thermal Stability of $LiNi_{1/3}Mn_{1/3}Co_{1/3-z}Mg_zO_2$, $LiNi_{1/3-z}Mn_{1/3}Co_{1/3}Mg_zO2$, and $LiNi_{1/3}Mn_{1/3-z}Co_{1/3}Mg_zO_2$†, Chem. Mater., 22 (2010) 1164-1172.

[16] P. Yue, Z. Wang, H. Guo, X. Xiong, X. Li, A low temperature fluorine substitution on the electrochemical performance of layered $LiNi_{0.8}Co_{0.1}Mn_{0.1}O_{2-z}F_z$ cathode materials, Electrochim. Acta, 92 (2013) 1-8.

[17] S.H. Park, S.S. Shin, Y.K. Sun, The effects of Na doping on performance of layered $Li_{1.1-x}Na_x(Ni_{0.2}Co_{0.3}Mn_{0.4})O_2$ materials for lithium secondary batteries, Materials Chemistry and Physics, 95 (2006) 218-221.

[18] A. Milewska, M. Molenda, J. Molenda, Structural, transport and electrochemical properties of $LiNi_{1-y}Co_yMn_{0.1}O_2$ and Al, Mg and Cu-substituted $LiNi_{0.65}Co_{0.25}Mn_{0.1}O_2$ oxides, Solid State Ionics, 192 (2011) 313-320.

[19] L. Liao, X. Wang, X. Luo, X. Wang, S. Gamboa, P.J. Sebastian, Synthesis and electrochemical properties of layered $Li(Ni_{0.333}Co_{0.333}Mn_{0.293}Al_{0.04})O_{2-z}F_z$ cathode materials prepared by the sol–gel method, J. Power Sources, 160 (2006) 657-661.

[20] Q. Liu, K. Du, H. Guo, Z.-d. Peng, Y.-b. Cao, G.-r. Hu, Structural and electrochemical properties of Co–Mn–Mg multi-doped nickel based cathode materials $LiNi_{0.9}Co_{0.1-x}(Mn_{1/2}Mg_{1/2})_xO_2$ for secondary lithium ion batteries, Electrochim. Acta, 90 (2013) 350-357.

[21] Y. Huang, J. Chen, J. Ni, H. Zhou, X. Zhang, A modified ZrO2-coating process to improve electrochemical performance of $LiNi_{1/3}Co_{1/3}Mn_{1/3}O_2$, Journal of Power Sources, 188 (2009) 538-545.

[22] J. Lu, Q. Peng, W. Wang, C. Nan, L. Li, Y. Li, Nanoscale coating of LiMO2 (M = Ni, Co, Mn) nanobelts with Li+-conductive Li2TiO3: toward better rate capabilities for Li-ion batteries, Journal of the American Chemical Society, 135 (2013) 1649-1652.

[23] C.-H. Lu, Y.-K. Lin, Microemulsion preparation and electrochemical characteristics of $LiNi_{1/3}Co_{1/3}Mn_{1/3}O_2$ powders, Journal of Power Sources, 189 (2009) 40-44.

[24] N.N. Sinha, N. Munichandraiah, Synthesis and characterization of carbon-coated $LiNi_{1/3}Co_{1/3}Mn_{1/3}O_2$ in a single step by an inverse microemulsion route, ACS applied materials & interfaces, 1 (2009) 1241-1249.

[25] S.K. Jeong, K.S. Nahm, A.M. Stephan, Synthesis of $Li(Co_{0.8}Ni_{0.2-y}Al_y)O_2$ ($y \leq 0.02$) by combustion method as a possible cathode material for lithium batteries, Materials Science and Engineering: A, 445-446 (2007) 657-662.
[26] F. Zhou, X. Zhao, C. Goodbrake, J. Jiang, J.R. Dahn, Solid-State Synthesis as a Method for the Substitution of Al for Co in $LiNi_{1/3}Mn_{1/3}Co_{1/3-z}Al_zO_2$, Journal of The Electrochemical Society, 156 (2009) A796.
[27] F. Zhou, X. Zhao, Z. Lu, J. Jiang, J.R. Dahn, The effect of Al substitution on the reactivity of delithiated $LiNi_{1/3}Mn_{1/3}Co_{1/3-z}Al_zO_2$ with non-aqueous electrolyte, Electrochemistry Communications, 10 (2008) 1168-1171.
[28] F. Zhou, X. Zhao, J.R. Dahn, Synthesis, Electrochemical Properties, and Thermal Stability of Al-Doped $LiNi_{1/3}Mn_{1/3}Co_{1/3-z}Al_zO_2$ Positive Electrode Materials, Journal of The Electrochemical Society, 156 (2009) A343.
[29] H. Ren, X. Li, Z. Peng, Electrochemical properties of $Li(Ni_{1/3}Mn_{1/3}Al_{1/3-x}Co_x)O_2$ as a cathode material for lithium ion battery, Electrochimica Acta, 56 (2011) 7088-7091.
[30] F. Zhou, X. Zhao, Z. Lu, J. Jiang, J.R. Dahn, The Effect of Al Substitution on the Reactivity of Delithiated $LiNi_{0.5-z}Mn_{0.5-z}A1_{2z}O_2$ with Nonaqueous Electrolyte, Electrochemical and Solid-State Letters, 11 (2008) A155.
[31] L. Croguennec, J. Bains, J. Bréger, C. Tessier, P. Biensan, S. Levasseur, C. Delmas, Effect of Aluminum Substitution on the Structure, Electrochemical Performance and Thermal Stability of $Li_{1+x}(Ni_{0.40}Mn_{0.40}Co_{0.20-z}Al_z)_{1-x}O_2$, Journal of The Electrochemical Society, 158 (2011) A664.
[32] Y. Ding, P. Zhang, Z. Long, Y. Jiang, F. Xu, Morphology and electrochemical properties of Al doped $LiNi_{1/3}Co_{1/3}Mn_{1/3}O_2$ nanofibers prepared by electrospinning, Journal of Alloys and Compounds, 487 (2009) 507-510.
[33] T. Ohzuku, Atsushi Ueda, M. Nagayama, Electrochemistry and Structural Chemistry of $LiNiO_2$ (R3m) for 4 Volt Secondary Lithium Cells, J. Electrochem. Soc., 140 (1993) 1862-1869.
[34] T.E. Conry, A. Mehta, J. Cabana, M.M. Doeff, Structural Underpinnings of the Enhanced Cycling Stability upon Al-Substitution in $LiNi_{0.45}Mn_{0.45}Co_{0.1-y}Al_yO_2$ Positive Electrode Materials for Li-ion Batteries, Chem. Mater., 24 (2012) 3307-3317.